PLOS ONE

RESEARCH ARTICLE

Perfluorocarbon-Loaded Lipid Nanocapsules to Assess the Dependence of U87-Human Glioblastoma Tumor pO_2 on *In Vitro* Expansion Conditions

Laurent Lemaire[1,2]*, Janske Nel[1,2], Florence Franconi[3], Guillaume Bastiat[1,2], Patrick Saulnier[1,2]

1 INSERM U 1066, 'Micro et Nanomédecines biomimétiques - MINT', Angers, France, **2** Université Angers, UMR-S1066, Angers, France, **3** PRIMEX-IRM, Université d'Angers, Angers, France

* laurent.lemaire@univ-angers.fr

CrossMark
click for updates

OPEN ACCESS

Citation: Lemaire L, Nel J, Franconi F, Bastiat G, Saulnier P (2016) Perfluorocarbon-Loaded Lipid Nanocapsules to Assess the Dependence of U87-Human Glioblastoma Tumor pO_2 on *In Vitro* Expansion Conditions. PLoS ONE 11(10): e0165479. doi:10.1371/journal.pone.0165479

Editor: Gabriele Multhoff, Technische Universitat Munchen, GERMANY

Received: April 25, 2016

Accepted: October 12, 2016

Published: October 27, 2016

Copyright: © 2016 Lemaire et al. This is an open access article distributed under the terms of the Creative Commons Attribution License, which permits unrestricted use, distribution, and reproduction in any medium, provided the original author and source are credited.

Data Availability Statement: All relevant data are within the paper.

Funding: This work was supported by 'Comité Inter-Régional Grand Ouest de La Ligue Contre le Cancer' (CIRGO). The funders had no role in study design, data collection and analysis, decision to publish, or preparation of the manuscript.

Competing Interests: The authors have declared that no competing interests exist.

Abbreviations: ^{19}F-oximetry, Fluorine oximetry; ASL, Arterial Spin Labeling; BSA, Bovine Serum

Abstract

Growing tumor cell lines, such as U87-MG glioma cells, under mild hypoxia (3% O_2) leads to a ca. 40% reduction in growth rate once implanted in the brain of nude mice, as compared to normoxia (21% O_2) grown cells, wherein the former over-express HIF-1 and VEGF-A. Despite developing differently, the tumors have similar: blood perfusion, oxygen consumption, and vascular surface area parameters, whereas the number of blood vessels is nearly doubled in the tumor arising from normoxia cultured cells. Interestingly, tumor oxygen tension, measured using ^{19}F-oximetry, showed that the normoxia grown cells led to tumors characterized by mild hypoxic environment (approximately 4%) conditions, whilst the hypoxia grown cells led to tumors characterized by physioxic environment (approximately 6%) conditions. This reversal in oxygen concentration may be responsible for the apparent paradoxical growth profiles.

Introduction

Most of the studies dealing with glioblastoma cell lines are performed with cells cultured at atmospheric oxygen concentration (i.e. 21% O_2), despite the fact that brain tissue oxygenation hosting the aforementioned tumoral cells is always lower, and as soon as the tumor proliferates the pO_2 decreases further, thus tending towards zero within its necrotic center [1–4].

Over the past years, the issue of the 'appropriate' oxygen tension to culture glioma cell lines or glioma stem cells has emerged as an important issue as the phenotype of the cells can be radically modified with oxygenation [5]. Such changes include: the significant alteration of HIF-1 expression in high oxygen concentrations [6,7]; the reduction of CD133 expression [8,9]; alterations in the expression of numerous genes involved in angiogenesis or metabolic reprogramming [10,11] and therefore in cellular metabolic profiles [12,13]; as well as a possible impact on therapeutic intervention, such as photodynamic therapy [14]. However, these modifications

Albumin; CA9, Carbonic Anhydrase 9; DAPI, 4',6-Diamidino-2-Phenylindole; DMEM, Dulbecco's Modified Eagle's Medium; FCS, Fetal Calf Serum; FISP, Fast Imaging with Steady-State Precession; FITC, Fluorescein; HASTE, Half-Fourier Acquisition Single-Shot Turbo Spin-Echo; HIF-1, Hypoxia-inducible Factor 1; HPRT1, Hypoxanthine-guanine Phosphoribosyltransferase 1; Kolliphor, Kolliphor® HS15; Lipoïd, Lipoïd® S75-3; MMP2, Matrix Metalloproteinase 2; OCT4, Octamer Binding Protein 4; PBS, Phosphate Buffered Saline; PFA, Paraformaldehyde; PFCE, Perfluoro-15-crown-5-ether; RARE, Rapid Acquisition with Relaxation Enhancement; TBF, Tumor Blood Flow; VEGF-A, Vascular Endothelial Growth Factor A.

can be transitory and may be attenuated or reversed once the cells are implanted in animals for subsequent *in vivo* studies. Indeed, the fate of the cells after stereotactic inoculation in the mouse brain appears heterogeneous. Kathagen et al. [10] described a glioblastoma stem-like tissue cell line from a patient biopsy, cultured under hypoxia (1% O_2), which grew faster as compared to its culture under atmospheric oxygen tension (21%). The same fate was reported by Bourseau-Guilmain et al. [8] for one grade IV glioblastoma cell line arising from a patient biopsy, but also the reverse situation for another grade IV glioblastoma cell line, i.e. the fastest growth being observed for the cells cultured under atmospheric (21% O_2) conditions upon implantation in mice. This latest observation was also done with the established U87-MG cell line [13].

Currently, the impact of oxygen tension concentration during cell culture, and the physiology of the subsequent brain tumor, is not extensively documented. With the present study, we are reporting the *in vivo* characterization of a U87-MG tumor model initially expanded under mild (3%) or atmospheric oxygen (21%) conditions, in terms of blood perfusion and oxygenation. Data were obtained using magnetic resonance (MR) imaging, respectively; arterial spin labelling (ASL) [15] and fluorine oximetry (^{19}F-oximetry) using dedicated oxygen nanosensors [16].

Materials and Methods

Perfluoro-15-crown-5-ether loaded lipid nanocapsules formulation

Perfluoro-15-crown-5-ether (PFCE) loaded lipid nanocapsules (LNCs) (thus PFCE-LNC) were prepared as previously described using a phase-inversion process [16,17]. Briefly, the quantities of the PFCE (oil phase), water and NaCl (aqueous phase), Kolliphor® HS15 and Lipoïd (surfactants) were precisely weighed: m_{PFCE} = 5 g, $m_{Kolliphor}$ = 2.115 g, $m_{Lipoïd}$ = 0.188 g, m_{Water} = 5 g and m_{NaCl} = 0.5 g. A four step process was performed to obtain PFCE-LNCs: to dissolve the Lipoïd within the initial solution, the temperature was increased from standing room temperature to 95°C, where after a 1 minute sonication, using a Microson XL2007 sonication probe set at 10 W (Misonix, Farmingdale, USA) was performed, prior to three heating and cooling cycles from 25°C to 95°C. Upon the final cooling, once the temperature reached 70°C, a rapid cold dilution was performed by adding 3.5 mL of cold (4°C) milli-Q water.

Lipoïd® S75-3 (soybean lecithin– 69% phosphatidylcholine and 10% phosphatidylethanolamine) and Kolliphor® HS15 were supplied by Lipoïd GmbH (Ludwigshafen, Germany) and BASF (Ludwigshafen, Germany), respectively. Perfluoro-15-crown-5-ether ($C_{10}F_{20}O_5$) was provided by Chemos GmbH (Regenstauf, Germany). NaCl was purchased from Prolabo (Fontenay-sous-bois, France). Deionized water was obtained from a Milli-Q plus® system (Millipore, Bilerica, USA).

In vitro conditions for U87-MG cells expansion

All experiments were performed with cells between passages 12 and 15. The U87-MG cell line was provided by the ATCC (LGC Promochem, Molsheim, France) and grown in Dulbecco's modified Eagle's medium high glucose (Lonza, Verviers, Belgium) supplemented with 10% fetal calf serum (FCS) (HABS; EFS, Lyon, France) and 1% antibiotic solution (Sigma-Aldrich, Saint Quentin Fallavier, France) at 37°C in a humidified incubator under an atmosphere containing 5% CO_2, and either 3% or 21% O_2.

Orthotopic transplantation of U87-MG cells into mouse brain

Animal care and use were in strict accordance with the regulations of the French Ministry of Agriculture and approved by the Pays de la Loire Ethics in Animal Experimentation

Committee under project number 01858.03. The manuscript does not contain patient data. Brain tumors were induced via the stereotaxic inoculation of U87-MG human glioma cells in 7–8 week-old female nude mice (Charles Rivers, France) as previously described [18]. Briefly, under Rompun® (Xylazine, Bayer AG, Leverkusen, Germany) and Clorketam® (Kétamine, Vétoquinol, Lure, France) anesthesia, mice were fixed in a stereotaxic holder and placed on a heating pad to maintain the appropriate physiological temperature. Through a 1mm drilled hole in the skull (anterior −0.5 mm, lateral 2.5 mm, depth −3.5 mm according to the bregma), a 5 μL suspension of 7.5 x 10^4 U87-MG glioma cells, grown at either 3 or 21% O_2, were injected over a 10-minute period into the caudate putamen of the right hemisphere. After surgery, mice received a single 15μg/kg subcutaneous injection of Vetergesic® (buprenorphin, Sogeval, France) and were monitored daily for mobility and grooming until their participation in the imaging protocol. Two groups of 18 mice were inoculated with cells grown at either 3 or 21% O_2. Each group was subdivided into two; 6 mice were dedicated to tumor blood flow measurements and histological analysis and 12 mice for tumor oxygenation measurements.

In vivo measurement of brain tumors volume and perfusion

MR imaging was performed using a 7T scanner (Biospec 70/20 Avance III, Bruker Wissembourg, France) equipped with BGA12S gradient system (675mT/m). Animal body temperature was maintained throughout the experiment by hot water circulation in an animal bed. During the MR protocol, mice were anesthetized with 0.5% of isoflurane and respiration was monitored. Tumor volume was assessed over time using a ^{1}H cryoprobe and a rapid acquisition with relaxation enhancement (RARE) sequence (TR = 3,200 ms; effective echo time (T_{Eeff}) = 21.3 ms; acceleration factor = 4; FOV = 2×2 cm; matrix 256 × 256; nine contiguous slices of 0.5 mm, Nex = 1). Volumes were calculated from manually drawn region of interest. The tumor volume growth curves were subsequently fitted by the method of least squares with an exponential function and the time constant of the exponential converted into a doubling time value [13]. Tumor perfusion was assessed by a segmented Fast Imaging with Steady-State Precession arterial spin labeling sequence (FISP-ASL). Homogeneous radiofrequency excitation was achieved using a proton volume resonator (diameter 87 mm, homogeneous length 80 mm) and signal reception was performed with an actively decoupled phased array surface coil (4 channels). Blood flow was measured from two T1 maps acquired once with slice-selective inversion and once with global inversion [15]. A series of 40 gradient echoes were acquired after the inversion pulse to acquire T1 maps (flip angle = 8°, echo time = 1.8 ms, field of view = 18 mm x 18 mm, matrix size = 128 x 128, excitation hermite pulse duration = 800 μs, inversion hyperbolic secant pulse duration = 15 ms, imaging slice thickness = 1.5 mm, labeling slice thickness = 3.9 mm, with the first echo started 20 ms after the inversion pulse and the duration between each echoes lasting 60 ms). 32 segments were used to fill k-space. A repetition delay of 13 s was introduced after the acquisition of a set of gradient echoes to allow for full relaxation between two inversion pulses. The total measurement time lasted approximately 14 min. Tumoral blood flow (TBF) was calculated with ParaVision 5.1 software (Bruker, Wissembourg, France). At this stage, tumors did not induce any evident discomfort to the mice as assessed by mobility or grooming. At the end of the imaging protocols, the animals were sacrificed.

In vivo measurement of brain tumors oxygenation

When the tumors were approximately 10 μL in volume, the mice underwent an intra-tumoral stereotactic injection of 8 μL PFCE-LNCs, using a convection-enhanced delivery protocol [19]. The fluorine acquisitions were performed using a 40 mm ^{1}H/^{19}F birdcage. The geometrical parameters were fixed at FOV = 2 x 2 cm, matrix 64 x 36 zero-filled to 64 x 64, slice thickness = 4

mm, and one average was performed. A Half-Fourier Acquisition Single-Shot Turbo Spin-Echo (HASTE) sequence (RARE factor = 36, TE = 4.6 ms, TR = 6 s) with 16 inversion times ranging between 30 ms to 3500 ms was used to produce T1 maps which were converted into tumoral pO_2 as previously reported [16].

PO_2 was assessed on anaesthetized mice (0.5% of isoflurane) at rest, i.e. animals breathing air, as well as after a 20 minute challenge with O_2. Upon switching back to air, tumor pO_2 was measured over time, and the profile of the pO_2 change was then fitted with a mono-exponential function whose time constant mainly reflected tumor oxygen consumption [20,21].). At this stage, tumors did not induce any evident discomfort to the mice as assessed by mobility or grooming. At the end of the imaging protocols, the animals were sacrificed.

Immunofluorescence

Brain cryosections were air-dried, rehydrated in phosphate buffered saline (PBS) and fixed for 10 min in 4% paraformaldehyde (PFA), pH 7.4, at 4°C. To block non-specific binding, the sections were incubated in PBS containing 4% bovine serum albumin (BSA) and 10% normal goat serum. The sections were incubated overnight at 4°C with isotype controls and primary antibodies against endothelial cells (mouse CD31; BD Biosciences) and proliferative cells (Ki67; Dako). Primary antibodies were detected using biotinylated secondary antibody and the signal amplified using streptavidin—fluorescein (streptavidin-FITC) (Dako, les Ullis, France). Nuclei were counterstained with 4',6-diamidino-2-phenylindole (DAPI) (Sigma-Aldrich, Saint Quentin Fallavier, France). Cryosections from 3 mice of each group (3% or 21% O_2 initially grown U87-MG) were analyzed under a fluorescence microscope (Axioscope 2 optical, Zeiss, LePecq, Germany). The numbers of CD31 positive vessels and Ki 67 positive cells were counted using the MetaView computerized image-analysis system for three brain cryosections per mouse. Two-four fields/cryosection, at × 200 magnification, were randomly chosen in the tumor. The results are expressed as the mean number of positively stained vessels/mm^2 for each group ±IC95%.

RNA isolation, cDNA synthesis and quantitative real-time PCR

Total RNAs were extracted from U87-MG glioblastoma tumors using the *RNeasy* Mini *Kit* (Qiagen). Briefly, 1 μg of RNA was reverse-transcribed into complementary DNA using random primers and *Superscript II* according to the manufacturer's recommendations (Invitrogen, Life Technologies, Thermo Fisher Scientific). Quantitative real-time PCR was performed using the *sybrgreen* Master mix (Thermo Fisher Scientific) and the LightCycler 480 (Roche Diagnostics) according to the manufacturer's instructions. Primer pairs used for each transcript were specifically designed using Primer Blast software. The relative abundance of mRNA levels was calculated using the $2^{-\Delta\Delta Ct}$ method for each gene using hypoxanthine-guanine phosphoribosyltransferase 1 (HPRT1) gene Ct values for normalization. Five mRNA levels were evaluated: endothelial growth factor A (VEGFA) involved in angiogenesis, the carbonic anhydrase 9 (CA9) and pyruvate dehydrogenase kinase 1 (PDK1) involved in metabolic reprogramming, of urokinase receptor (UPAR) and matrix metalloproteinase 2 (MMP2) involved in invasion and metastasis.

Statistical analysis

All quantitative data are represented as mean± standard error of the mean, and the statistical significance was determined using *t*-test. Differences were considered significant if the p value was < 0.05.

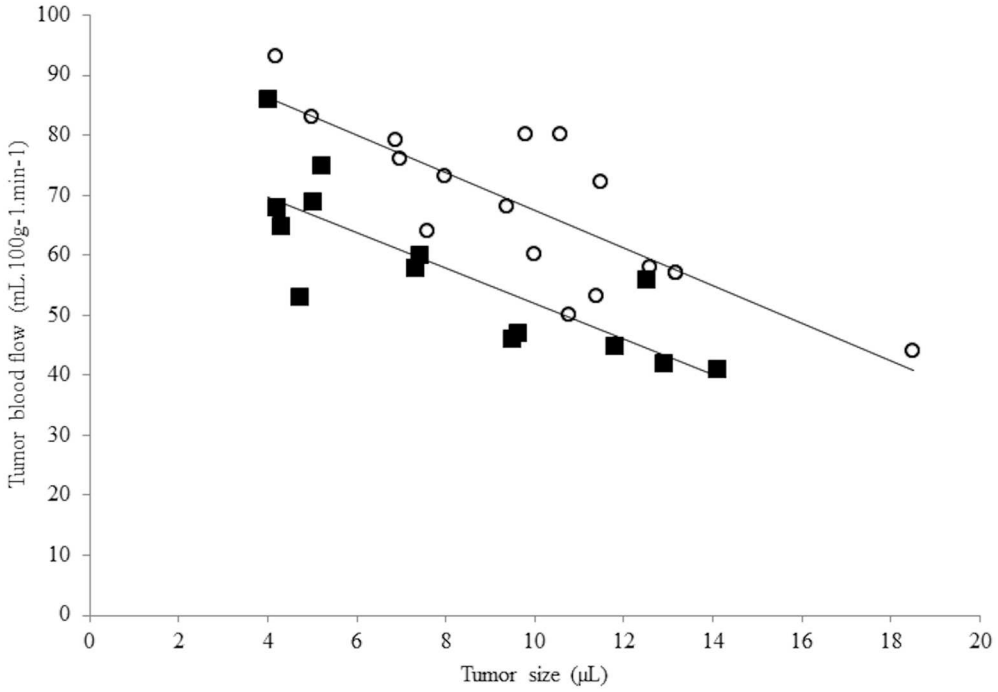

Fig 1. Tumor blood flux as a function of tumor size. This figure illustrates the impact of the tumor size on the tumoral blood flow. Open circles (o) correspond to data acquired in the group arising from the cells initially grown under mild hypoxia (3% O_2) and close squares (■) to data acquired in the group arising from the cells initially grown under normoxia (21% O_2).

doi:10.1371/journal.pone.0165479.g001

Results

Growing U87-MG cells under mild hypoxic conditions, prior to cell implantation within mice brain, impacts subsequent growth *in vivo* [13]. In the present study, this observation was confirmed as the tumor volume doubling time after stereotactic implantation in nude mice brain was calculated at 3.7 ± 0.4 versus 2.0 ± 0.2 days (n = 6 in each group, $p < 0.001$) when cells were proliferated under 3% or 21% O_2, respectively.

A fast and non-invasive characterization of the tumor perfusion can be gained using ASL-MR imaging. As shown in Fig 1, it appears that the perfusion is dependent on the size of the tumor in both tumor groups, with a reduction of approximately 3 mL/min/100g of the Tumor Blood Flow (TBF) when the tumor volume increases by 1 μL. As a consequence, tumors were sized matched in the present study. The average tumor size for the hypoxic group (3% O_2) was 7.1 ± 0.5 μL and 7.5 ± 0.5 for the normoxic group (21% O_2). Under those circumstances, the measured TBF was not significantly different with values of $TBF_{3\%}$ = 69 ± 4 mL/min/100g and $TBF_{21\%}$ = 68 ± 5 mL/min/100g for each respective groups (p = 0.79).

Nevertheless, despite the absence of difference between both groups in terms of TBF, the histological analysis of the brain tumors showed that the number of vessels was significantly reduced in the 3% group, i.e. $n_{3\%}$ = 660 ± 51 vessels/mm² versus $n_{21\%}$ = 919 ± 35 vessels/mm² ($p < 0.001$). Notably, the vessels tended to be larger in the 3% group (p = 0.03), with an average surface area of $S_{3\%}$ 48 ± 5 μm² versus $S_{21\%}$ 33 ± 2 μm² in the 21% group (Fig 2). Thus the vascular surface area, defined as the number of vessels/mm² multiplied by the average surface of the vessels, is not significantly different within the two types of tumors and represents ca. 3% of the tumoral tissue surface. In terms of the mRNA level of vascular endothelial growth factor A (VEGF-A), carbonic anhydrase 9 (CA9), pyruvate dehydrogenase kinase (PDK1), urokinase

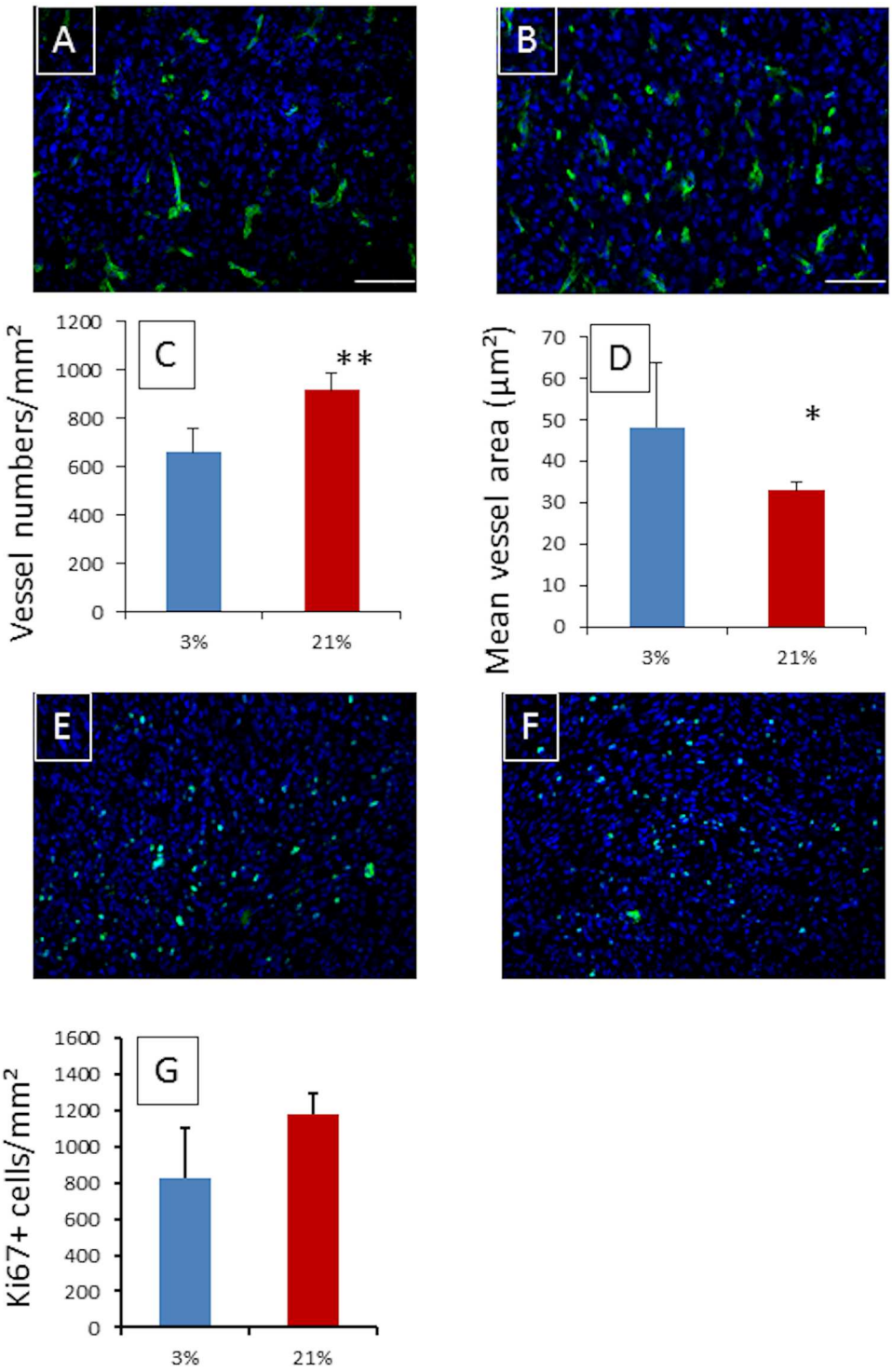

Fig 2. Blood vessel density and cell proliferation assessment with respect to the tumor group explored. Immunofluorescence staining of CD31 and Ki67 in a typical tumor arising from mild hypoxic (3% O_2) grown U87-MG cells ((A)—CD31 / (E)–Ki67) and from normoxic grown (21% O_2) tumor ((B)—CD31 / (F)–Ki67) once a size of 8µL is reached. Nucleus staining was performed using DAPI (Blue). Scale bar = 100µm. Quantitative vessel density analysis (C) and average vessel area (D) revealed, on average, 668 ± 50 vessels/mm with an area of 46 ± 5 μm^2 in the tumor arising from the cells cultured under mild hypoxia versus 919 ± 35 vessels/mm^2 with an area of 33 ± 2 μm^2 in the tumor arising from cells cultured under normoxia [$p<0.001$ for vessel number (**) and $p<0.03$ for area (*)]. However, the vascular surface

average is not significantly different between both groups and is ~3%. The quantitative analysis of Ki67 positive cells is presented in frame (G), and despite non-significant ($p = 0.107$) on average, 829 ± 138 positive cells/mm^2 were counted in the tumor arising from the cells cultures in mild hypoxia condition versus 1178 ± 59 positive cells/mm^2 in the tumor arising from cells cultured under normoxia.

doi:10.1371/journal.pone.0165479.g002

receptor (UPAR), matrix metalloproteinase 2 (MMP2), vimentin (VIM) or octamer binding protein 4 (OCT4), an over-expression in the 3% and 21% tumors was measured in comparison to the contralateral brain. However, the comparison between the two groups of tumors only showed a limited 3-fold over-expression in CA9 and a 2-fold over-expression in PKD1, in the 21% O_2 tumor group as compared to the 3% O_2.

In order to assess the tumoral oxygenation, an intratumoral injection of perfluorocarbon-loaded nanocapsules was performed as previously described [16]. The pO_2 value measured at rest, i.e. isoflurane anesthesia with spontaneous air breathing, within the mice bearing U87-MG brain tumor initially cultured under 3% pO_2 was equal to $pO_{2\text{-Air}}^{3\%} = 47 \pm 3$ mmHg ($n = 12$). In the 21% group, the value is significantly reduced ($p < 0.01$) as $pO_{2\text{-Air}}^{21\%} = 33 \pm 3$ mmHg ($n = 12$) (Fig 3). After 20 minutes the O_2 challenge, the measured values for both groups tended towards 100mmHg. Thus fitting the profile of the pO_2 change over time with a mono-exponential function showed that tumor oxygen consumption, represented by the time constant of the function, is not significantly different ($p = 0.4$) as values are $k_{3\%} = 0.35 \pm 0.10$ min^{-1} and $k_{21\%} = 0.42 \pm 0.13$ min^{-1}.

Discussion

The impact of cell phenotype changes, induced by oxygen tension during *in vitro* expansion prior to implantation in living systems, is currently under debate with respect to the pertinence of the models used [5,22], and the potential phenotype reversal/adaptation once the model is hosted in the living environment whose tissular oxygen tension may range from almost 0% up

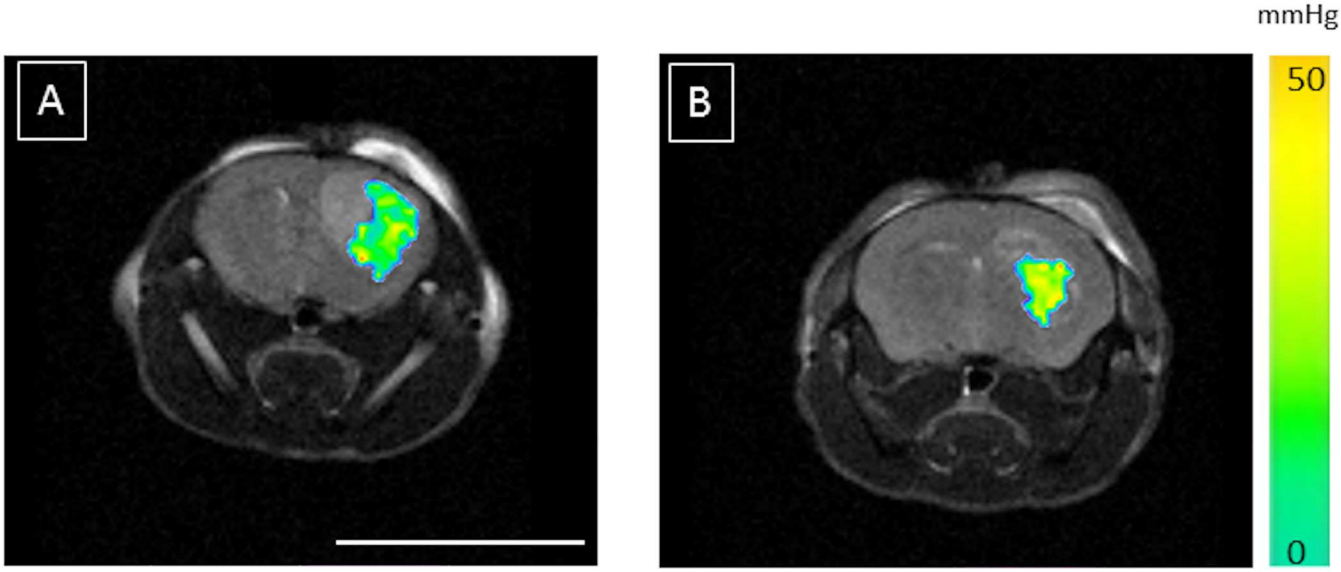

Fig 3. Tumor pO_2 assessed using perfluorocarbon loaded lipid nanocapsules. The average pO_2 value of the tumor arising from the cells cultured under mild hypoxia (3% O_2) (A) is measured at 47 ± 3 mmHg (ca. 6.2% O_2) whereas a value of 33 ± 3 mmHg is measured (ca. 4.3% O_2) in the tumor arising from cells cultured under normoxia (21% O_2) (B) ($p < 0.01$). Those values were measured under isoflurane anesthesia and spontaneous air breathing. Scale bar = 1cm.

doi:10.1371/journal.pone.0165479.g003

to 15% [3,23]. In the peculiar case of the widely used U87-MG glioma cell line for chemo-therapeutic assessments, cellular therapeutics, and MR methodological purposes [24–26], the impact of the initial culture conditions is often not recognized as a changeable parameter, even though we recently showed that the expansion of this cell line under moderate hypoxia (3% O_2) or under normoxia (21% O_2) led to significant modifications in tumor growth [13]. This observation is repeated in the present study. In order to understand the physiological causes of this differential growth, the vascularization of both types of tumor was assessed using non-invasive ASL-MRI and invasive histology. Tumor pO_2 was also measured using specially designed fluorinated nanosensors [16].

It is now well established that, irrespective of the type of the solid tumor explored, the tumor blood flow (TBF) is dependent on tumor size [27,28]. In this study, this observation was repeated (Fig 1), and in pursuance of comparisons between the two groups, tumors were size matched. Contrary to what Fig 1 portrays, i.e. that TBF tends to be higher in the 3% group as compared to the 21% O_2 group; the TBF of the tumor sized matched groups at ca. 7–8 μL was not significantly different. Indeed, TBF were measured at $TBF_{3\%}$ = 69 ± 4 mL/min/100g and $TBF_{21\%}$ = 68 ± 5 mL/min/100g ($p = 0.79$). Nevertheless, the invasive histological analysis of the tumors showed significant microscopic differences between the two groups. As shown in Fig 2, tumors arising from cells initially grown under mild hypoxia have significantly larger blood vessels, with on average a surface of $S_{3\%}$ = 46 ± 5 μm^2 versus $S_{21\%}$ = 33 ± 2 μm^2 in the 21% group ($p = 0.03$), but the number of vessels is significantly reduced $n_{3\%}$ = 660 ± 51 vessels/mm^2 versus $n_{21\%}$ = 919 ± 35 vessels/mm^2 ($p < 0.001$), leading to similar vascular surface area, ca. 3%, possibly explaining why the TBF between the two groups are not dissimilar. However, the vessel density results appear contradictory according to our previous work regarding the *in vitro* evaluation of the hypoxia impact on the cell phenotype [13]. Indeed, *in vitro* mild hypoxia led to the stabilization of HIF-1 and subsequently the over-expression of VEGF-A. As a consequence, we would have expected better angiogenesis in tumors arising from cells initially grown under mild hypoxia. However, a hypothesis involving the oxygen pressure in the host tissue where the cells were implanted, i.e. the rodent striatum, could be proposed. Indeed, a recent report has shown that average oxygen saturation reaches a value of 67% in the rat cortex and 59% in the rat striatum [2,29]. These values can be converted into local oxygen pressures of 50 mmHg (i.e. 6.5% O_2) and 44 mmHg (5.7% O_2), respectively, using the Hill equation, wherein n = 2.6 and P_{50} = 38 mmHg [2]. It is therefore possible that an increase in oxygen pressure affecting the cells (rising from 3% oxygen during culturing to ca. 6% in the host tissue) could lead to a switching off of the HIF-1 pathway as previously reported on Hela [30] and Caco2 cells [11]. However, the mirror image of this hypothesis is reflected in the cells cultured under 21% oxygen; even if the oxygen pressure reduction in the host tissue exists, it should not be large enough to trigger the on/off switching of the pathway responsible for the increased angiogenesis. The qPCR analysis performed on the implanted tumors, upon reaching a size of ca. 8 μL, do not provide any support for this hypothesis as no difference in VEGF-A expression is observed between the two groups. However, this hypothesis may be too simplistic; it assumes that the host tissue pO_2 drives the tumoral cells phenotype from the cell inoculation and as well as throughout the tumor development. As a consequence, we have measured the tumoral pO_2 using ^{19}F-oximetry with specially designed fluorine loaded-nanocapsules [16]. Prior any discussion on the values measured using this method, it has to be noted that the pO2 measurement depend on the infusion zone of the probe within the tumor, and as shown in Fig 3 may not reflect the tumor pO2 of the entire tumor. However, this limitation is common to all methods using exogenous probes, as the distribution within the tumor may be dependent on tissue perfusion as well as on the capillary permeability for example. Nevertheless, we observed that tumors arising from the mild hypoxic cells had a higher pO_2 (Fig 3), within the sizes used for

this study, with values of $pO_{2\text{-}Air}^{3\%} = 47 \pm 3$ mmHg (ca. 6.2% O_2) versus $pO_{2\text{-}Air}^{21\%} = 33 \pm 3$ mmHg (ca. 4.3% O_2) ($p < 0.01$). Moreover, this difference in pO_2 cannot be attributed to a larger use of oxygen in the 21% tumor group as time constant for this process was defined within an oxygen challenge [21] is no different from the constant calculated for the 3% tumor group ($k_{21\%} = 0.42 \pm 0.13$ min^{-1} versus $k_{3\%} = 0.35 \pm 0.10$ min^{-1}, $p > 0.4$). Taken all together, the faster growth of the 21% group may result from the tumoral cells creating a local environment, characterized by a lower pO_2 and transferring the cells into a 'deeper mild hypoxic' environment which promotes tumor growth [31], regardless of whether they are implanted in the same physioxic environment as the 3% grown cells. The molecular analysis of the grown tumors cannot unambiguously sustain this observation as it was performed on a single sample from each tumor group. These results, along with the proliferative KI-67 staining experiment, although being not significant ($p = 0.107$), indicate that the number of proliferative cells is higher in the 21% group, thus adding to the narrative to explain the faster growth of the 21% tumor group.

Following this descriptive study of the macroscopic differences observed relating to hypoxic environments, the next step will be to define the exact biological mechanism(s) and the dynamics which underlays these paradoxical growth profiles as well as a systemic exploration of others glioblastoma cell lines.

Conclusions

Growing tumor cell lines such as U87-MG glioma cells under mild hypoxia (3% O_2) or normoxia (21% O_2) leads to a peculiar phenotype, with over-expression of VEGF-A which should facilitate the growth of hypoxic cells *in vivo*. However, a paradoxical phenomenon is observed as normoxia grown cells gave rise to tumors faster than the mild hypoxia grown cells. Tumor oxygen tension measured using ^{19}F-oximetry showed that in the former, mild hypoxic conditions are reached as tumors are growing whereas, for the latter, physioxic conditions are observed with tumor growth and may explain the paradoxical growth profile.

Acknowledgments

We would like to thank; Mr. J. Cayon for his technical assistance in qPCR, the members of the local animal facility for the housing and care provided for the animals, and Dr. D. Wecker (Bruker Biospin) for the MRI sequence implementation. Ethical standards: Animal care and use were in strict accordance with the regulations of the French Ministry of Agriculture and approved by the Pays de la Loire Ethics in Animal Experimentation Committee under project number 01858.03. The manuscript does not contain patient data.

Author Contributions

Conceptualization: LL.

Formal analysis: LL FF.

Funding acquisition: LL.

Investigation: LL FF.

Methodology: LL FF GB.

Writing – original draft: LL FF GB.

Writing – review & editing: LL JN FF GB PS.

References

1. Bourke VA, Zhao DW, Gilio J, Chang CH, Jiang L, Hahn EW, et al. Correlation of radiation response with tumor oxygenation in the Dunning prostate R3327-At1 tumor. Int J Radiat Oncol 2007; 67 (4):1179–1186.
2. Christen T, Lemasson B, Pannetier N, Farion R, Segebarth C, Remy C, et al. Evaluation of a quantitative blood oxygenation level-dependent (qBOLD) approach to map local blood oxygen saturation. NMR Biomed 2011; 24(4):393–403. doi: 10.1002/nbm.1603 PMID: 20960585
3. Erecinska M, Silver IA. Tissue oxygen tension and brain sensitivity to hypoxia. Resp Physiol 2001; 128 (3):263–276.
4. Hou HG, Nemani VK, Du GX, Montano R, Song R, Gimi B, et al. Monitoring oxygen levels in orthotopic human glioma xenograft following carbogen inhalation and chemotherapy by implantable resonator-based oximetry. International Journal of Cancer 2015; 136(7):1688–1696. doi: 10.1002/ijc.29132 PMID: 25111969
5. Csete M. Oxygen in the cultivation of stem cells. Ann Ny Acad Sci 2005; 1049:1–8.
6. Pouyssegur J, Dayan F, Mazure NM. Hypoxia signalling in cancer and approaches to enforce tumour regression. Nature 2006; 441(7092):437–443. doi: 10.1038/nature04871 PMID: 16724055
7. Semenza GL. Targeting HIF-1 for cancer therapy. Nat Rev Cancer 2003; 3(10):721–732. doi: 10.1038/nrc1187 PMID: 13130303
8. Bourseau-Guilmain E, Lemaire L, Griveau A, Hervouet E, Vallette F, Berger F, et al. In vitro expansion of human glioblastoma cells at non-physiological oxygen tension irreversibly alters subsequent in vivo aggressiveness and AC133 expression. International Journal of Oncology 2012; 40(4):1220–1229. doi: 10.3892/ijo.2011.1271 PMID: 22134773
9. Platet N, Liu SY, El Atifi M, Oliver L, Vallette FM, Berger F, et al. Influence of oxygen tension on CD133 phenotype in human glioma cell cultures. Cancer Letters 2007; 258(2):286–290. doi: 10.1016/j.canlet.2007.09.012 PMID: 17977646
10. Kathagen A, Schulte A, Balcke G, Phillips HS, Martens T, Matschke J, et al. Hypoxia and oxygenation induce a metabolic switch between pentose phosphate pathway and glycolysis in glioma stem-like cells. Acta Neuropathol 2013; 126(5):763–780. doi: 10.1007/s00401-013-1173-y PMID: 24005892
11. Bruning U, Fitzpatrick SF, Frank T, Birtwistle M, Taylor CT, Cheong A. NFkappaB and HIF display synergistic behaviour during hypoxic inflammation. Cellular and molecular life sciences: CMLS 2012; 69 (8):1319–1329. doi: 10.1007/s00018-011-0876-2 PMID: 22068612
12. Kucharzewska P, Christianson HC, Belting M. Global profiling of metabolic adaptation to hypoxic stress in human glioblastoma cells. PLoS ONE 2015; 10(1):e0116740. doi: 10.1371/journal.pone.0116740 PMID: 25633823
13. Lemaire L, Franconi F, Siegler B, Legendre C, Garcion E. In vitro expansion of U87-MG human glioblastoma cells under hypoxic conditions affects glucose metabolism and subsequent in vivo growth. Tumour Biology 2015.
14. Albert I, Hefti M, Luginbuehl V. Physiological oxygen concentration alters glioma cell malignancy and responsiveness to photodynamic therapy in vitro. Neurol Res 2014; 36(11):1001–1010. doi: 10.1179/1743132814Y.0000000401 PMID: 24923209
15. Kober F, Iltis I, Izquierdo M, Desrois M, Ibarrola D, Cozzone PJ, et al. High-resolution myocardial perfusion mapping in small animals in vivo by spin-labeling gradient-echo imaging. Magnet Reson Med 2004; 51(1):62–67.
16. Lemaire L, Bastiat G, Franconi F, Lautram N, Dan TDT, Garcion E, et al. Perfluorocarbon-loaded lipid nanocapsules as oxygen sensors for tumor tissue pO(2) assessment. European Journal of Pharmaceutics and Biopharmaceutics 2013; 84(3):479–486. doi: 10.1016/j.ejpb.2013.01.003 PMID: 23352843
17. Heurtault B, Saulnier P, Pech B, Proust JE, Benoit JP. A novel phase inversion-based process for the preparation of lipid nanocarriers. Pharm Res 2002; 19(6):875–880. PMID: 12134960
18. Lemaire L, Franconi F, Saint-Andre JP, Roullin VG, Jallet P, Le Jeune JJ. High-field quantitative transverse relaxation time, magnetization transfer and apparent water diffusion in experimental rat brain tumour. NMR Biomed 2000; 13(3):116–123. PMID: 10861992
19. Franconi F, Chapon C, Le Jeune JJ, Richomme P, Lemaire L. Susceptibility gradient quantization by MRI signal response mapping (SIRMA) to dephaser. Medical Physics 2010; 37(2):877–884. doi: 10.1118/1.3298019 PMID: 20229897
20. Diepart C, Jordan BF, Gallez B. A New EPR oximetry protocol to estimate the tissue oxygen consumption *in vivo*. Radiation Research 2009; 172:220–225. doi: 10.1667/RR1448.1 PMID: 19630526

21. Diepart C, Magat J, Jordan BF, Gallez B. In vivo mapping of tumor oxygen consumption using (19)F MRI relaxometry. NMR in Biomedicine 2011; 24(5):458–463. doi: 10.1002/nbm.1604 PMID: 20891023

22. Wion D, Christen T, Barbier EL, Coles JA. PO(2) matters in stem cell culture. Cell stem cell 2009; 5 (3):242–243. doi: 10.1016/j.stem.2009.08.009 PMID: 19733532

23. Sullivan M, Galea P, Latif S. What is the appropriate oxygen tension for in vitro culture? Molecular human reproduction 2006; 12(11):653. doi: 10.1093/molehr/gal081 PMID: 17008346

24. Aoki H, Takada Y, Kondo S, Sawaya R, Aggarwal BB, Kondo Y. Evidence that curcumin suppresses the growth of malignant gliomas in vitro and in vivo through induction of autophagy: role of Akt and extracellular signal-regulated kinase signaling pathways. Molecular pharmacology 2007; 72(1):29–39. doi: 10.1124/mol.106.033167 PMID: 17395690

25. Clavreul A, Guette C, Faguer R, Tetaud C, Boissard A, Lemaire L, et al. Glioblastoma-associated stromal cells (GASCs) from histologically normal surgical margins have a myofibroblast phenotype and angiogenic properties. The Journal of Pathology 2014; 233(1):74–88. doi: 10.1002/path.4332 PMID: 24481573

26. Mesti T, Savarin P, Triba MN, Le Moyec L, Ocvirk J, Banissi C, et al. Metabolic impact of anti-angiogenic agents on U87 glioma cells. PLoS ONE 2014; 9(6):e99198. doi: 10.1371/journal.pone.0099198 PMID: 24922514

27. Hwang SH, Cha J, Jo K, Jeong YH, Kim H, Cho A, et al. Correlation of tumor size and metabolism with perfusion in hepatocellular carcinoma using dynamic contrast enhanced CT and F-18 FDG PET-CT. Journal of nuclear medicine: official publication, Society of Nuclear Medicine 2015; 56(3-sup3):1330.

28. Kallinowski F, Schlenger KH, Runkel S, Kloes M, Stohrer M, Okunieff P, et al. Blood flow, metabolism, cellular microenvironment, and growth rate of human tumor xenografts. Cancer Res 1989; 49 (14):3759–3764. PMID: 2736517

29. Lemasson B, Christen T, Tizon X, Farion R, Fondraz N, Provent P, et al. Assessment of multiparametric MRI in a human glioma model to monitor cytotoxic and anti-angiogenic drug effects. NMR Biomed 2011; 24(5):473–482. doi: 10.1002/nbm.1611 PMID: 21674650

30. Jiang BH, Semenza GL, Bauer C, Marti HH. Hypoxia-inducible factor 1 levels vary exponentially over a physiologically relevant range of O2 tension. Am J Physiol 1996; 271(4 Pt 1):C1172–1180. PMID: 8897823

31. Grimes DR, Kannan P, McIntyre A, Kavanagh A, Siddiky A, Wigfield S, et al. The role of oxygen in avascular tumor growth. PLoS ONE 2016; 11(4):e0153692. doi: 10.1371/journal.pone.0153692 PMID: 27088720